

# Interface engineering of high-Mg-content MgZnO/BeO/Si for p-n heterojunction solar-blind ultraviolet photodetectors

H. L. Liang, Z. X. Mei,<sup>a)</sup> Q. H. Zhang, L. Gu, S. Liang, Y. N. Hou, D. Q. Ye, C. Z. Gu, R. C. Yu, and X. L. Du<sup>a)</sup>

*Beijing National Laboratory for Condensed Matter Physics, Institute of Physics, Chinese Academy of Sciences, Beijing 100190, People's Republic of China*

(Received 26 April 2011; accepted 5 May 2011; published online 31 May 2011)

High-quality wurtzite MgZnO film was deposited on Si(111) substrate via a delicate interface engineering using BeO, by which solar-blind ultraviolet photodetectors were fabricated on the n-MgZnO(0001)/p-Si(111) heterojunction. A thin Be layer was deposited on clean Si surface with subsequent *in situ* oxidation processes, which provides an excellent template for high-Mg-content MgZnO growth. The interface controlling significantly improves the device performance, as the photodetector demonstrates a sharp cutoff wavelength at 280 nm, consistent with the optical band gap of the epilayer. Our experimental results promise potential applications of this technique in integration of solar-blind ultraviolet optoelectronic device with Si microelectronic technologies.

© 2011 American Institute of Physics. [doi:[10.1063/1.3595342](https://doi.org/10.1063/1.3595342)]

Solar-blind materials based on wide band gap semiconductors such as AlGaN,<sup>1</sup> diamond,<sup>2</sup> and MgZnO (Refs. 3–11) have received tremendous attention due to their potential applications in solar-blind ultraviolet (UV) detection.<sup>12</sup> MgZnO is one of the most competitive candidates for its tunable band gap hopefully covering the whole solar-blind spectrum region, as well as its large exciton binding energy, and more importantly, much lower growth temperature than AlGaN, etc.

In our previous work, solar-blind 4.55 eV band gap wurtzite Mg<sub>0.55</sub>Zn<sub>0.45</sub>O components have been achieved on c-sapphire by radio-frequency plasma assisted molecular beam epitaxy (rf-MBE),<sup>6</sup> and photodetectors based on this material have been realized with a sharp cutoff wavelength at 270 nm and 277 nm, respectively.<sup>3,4</sup> For potential integration of MgZnO optoelectronic device with the well-developed Si microelectronic technologies, n-MgZnO/p-Si heterojunction solar-blind UV detector is also highly desirable. However, the epitaxial growth of high-quality MgZnO films on Si substrate is a challenge due to the formation of amorphous SiO<sub>x</sub> layer at the initial growth stage of oxides. The protection of clean Si surface from oxidation with a buffer layer plays a key role to achieve single-crystalline MgZnO thin film growth. A range of methods, including insertion of nonoxide layers such as TiN,<sup>10,13</sup> AlN,<sup>13</sup> and CaF<sub>2</sub>,<sup>11</sup> deposition of Zn (Ref. 14) and Mg (Refs. 9 and 15) metals, have been adopted previously either for ZnO or MgZnO epitaxy. Another challenge is to create a suitable epitaxial template for high-Mg-content MgZnO with solar-blind band gap. An interfacial layer with four-coordinated bonding configuration is essential to avoid the occurrence of phase separation in MgZnO,<sup>9,11</sup> which heavily restricts the increase in Mg content and the band gap. Cubic MgO and CaF<sub>2</sub> cannot work without the addition of wurtzite ZnO buffer layer<sup>9,11</sup> since they have either six-coordination or a mixture of eight- and four-coordinations. On the other hand, ZnO is undesirable in MgZnO solar-blind UV detector because of its strong re-

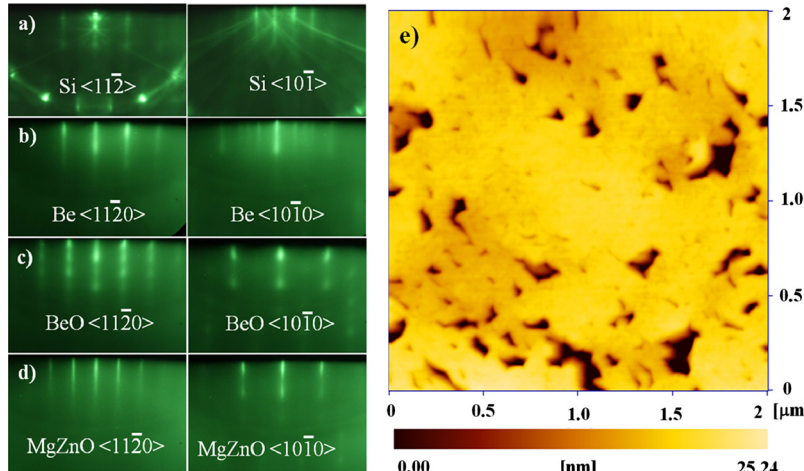
sponse to the longer UV wavelength. The shortest cutoff wavelength of MgZnO/Si photodetectors ever reported is ~300 nm,<sup>11</sup> still far away from the target of solar-blind detection.

In present work, a high-quality single-phase wurtzite MgZnO (0001) film with a solar-blind band gap was obtained on p-Si (111) substrate using Be and BeO interfacial layers to protect Si (111)-1 × 1 clean surface and to serve as a superior epitaxial template, respectively. A solar-blind UV photodetector was fabricated on this interface-engineered n-MgZnO/p-Si p-n heterojunction, which showed a well-defined rectifying behavior and a sharp cutoff wavelength at 280 nm, in a good agreement with the optical band gap determined by the reflectance spectroscopy measurement.

The wurtzite MgZnO film was grown on 2 in. p-Si (111) wafer by rf-MBE technique. The wafer was chemically cleaned by the regular RCA method and then thermally cleaned at 400 °C under ultrahigh vacuum condition. Deposition of a few nanometers thick Be layer was performed on Si (111)-1 × 1 surface at 200 °C, followed by an oxidation process at the same temperature. Growth of a quasihomo MgZnO buffer layer (~20 nm) and a high-Mg-content Mg-ZnO epilayer (350 nm) was subsequently carried out on the formed BeO layer. More details on this unique technique can be found elsewhere.<sup>6</sup> Note that the highest substrate temperature was kept below 400 °C during the whole growth procedure, which makes it possible to integrate the MgZnO optoelectronic device with the well-developed Si microelectronic technologies in future.

Reflection high-energy electron diffraction (RHEED) technique was efficiently utilized to *in situ* monitor the whole growth process. On Si (111)-1 × 1 clean surface [Fig. 1(a)], a thin Be (0001) layer was first deposited to prevent the surface from oxidation. It can be found that the Be layer has a 30° in-plane rotation of its lattice with respect to the substrate by a 3:1 domain matching [Fig. 1(b)]. In this way the in-plane lattice misfit can be lowered to ~3%, which benefits the formation of high-quality Be film. Note that it is not necessary to deposit the metal layer at a temperature as low as in the case of Mg on Si (Ref. 16) because the reaction of

<sup>a)</sup>Authors to whom correspondence should be addressed. Electronic addresses: zxmei@aphy.iphy.ac.cn and xldu@aphy.iphy.ac.cn.



Be and Si needs a considerable high temperature so that the interface between Be (0001)/Si (111) remains stable in this case. Oxidation with active oxygen radicals was then performed, and a thin single-crystalline BeO layer formed [Fig. 1(c)], which provides a good template for subsequent wurtzite MgZnO epitaxy. A MgZnO layer with low Mg content was grown to accommodate the large mismatch between BeO and high-Mg-content MgZnO layer. A single-phase wurtzite MgZnO film with nominally high Mg content was synthesized on the quasihomo MgZnO buffer layer, with a smooth surface as illustrated by the sharp streaky patterns in Fig. 1(d).

The surface morphology was further evaluated by atomic force microscopy (AFM) as shown in Fig. 1(e). The root mean square roughness in a  $10 \times 10 \mu\text{m}^2$  scanning area is about 1.56 nm (not shown here), demonstrating high crystal quality and smooth surface, which is consistent with the *in situ* RHEED observations. Moreover, the existence of small pits and jagged step edges, as seen in Fig. 1(e), implies a typical step-flow growth mode which has been reported in both GaN and Mg<sub>0.19</sub>Zn<sub>0.81</sub>O films grown at relatively high temperature.<sup>16,17</sup> This phenomenon is not usual for high-Mg-content MgZnO prepared at low temperature, which is presumably attributed to the interfacial layer playing a key role to change the growth dynamics of nucleation and relaxation of strain herein. The high crystal quality is thus naturally achieved meanwhile.

Further investigation on the interface structure was carried out by cross-sectional high resolution transmission elec-

FIG. 1. (Color online) RHEED patterns with incident electron beams along  $\langle 11\bar{2} \rangle_{\text{Si}}$  and  $\langle 10\bar{1} \rangle_{\text{Si}}$  azimuths, respectively, obtained from Si (111)-1  $\times$  1 surface (a); after Be deposition at 200 °C (b); after exposure of Be layer to oxygen radicals at 200 °C for 3 min (c); and after MgZnO epitaxial growth at 400 °C for 3 h (d); and AFM image of the wurtzite MgZnO epilayer in a  $2 \times 2 \mu\text{m}^2$  scanning area (e).

tron microscopy (HRTEM). Figure 2 shows the result taken along  $\langle 11\bar{2} \rangle_{\text{Si}}$  direction and its corresponding fast Fourier transformation (FFT). A well-defined interfacial layer can be clearly seen between the MgZnO layer and the Si substrate from Fig. 2(a). Figure 2(b) combined with the inset of Fig. 2(a) illustrates a wurtzite phase of BeO and a crystalline orientation relationship of  $[11\bar{2}0]_{\text{MgZnO}} \parallel [11\bar{2}0]_{\text{BeO}} \parallel [11\bar{2}]_{\text{Si}}$ , which agrees well with the *in situ* RHEED observations. It is worth to notice that the BeO interfacial layer has the same crystal structure with the MgZnO layer, demonstrating it is a suitable template for the epitaxial growth of single-crystalline wurtzite solar-blind MgZnO film with high Mg content.

To confirm the single-crystalline wurtzite nature of the epilayer, XRD  $\theta$ -2θ and  $\phi$ -scans were performed. Figure 3(a) shows the  $\theta$ -2θ scan result of the sample. The peak located at 35.04° is attributed to the diffraction from wurtzite

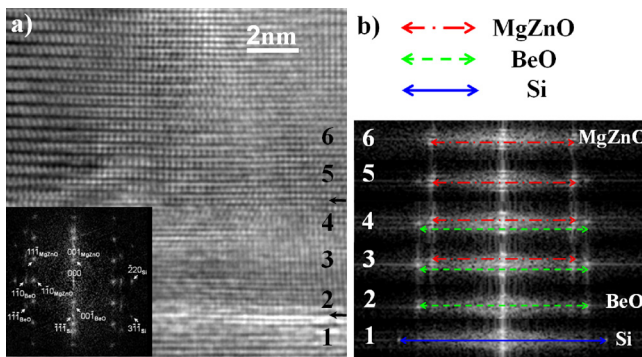


FIG. 2. (Color online) Cross-sectional HRTEM micrograph along  $\langle 11\bar{2} \rangle_{\text{Si}}$  direction near the interface region, whose FFT pattern is included as an inset (a); and the corresponding FFT patterns obtained from the different layers (b).

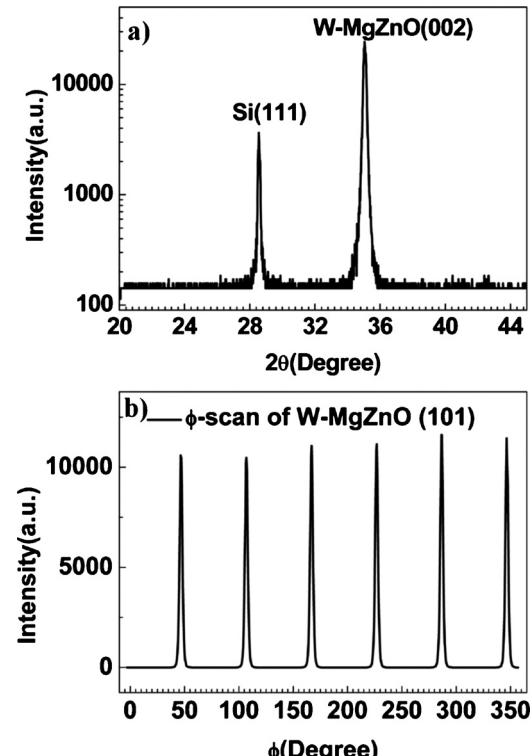


FIG. 3. XRD  $\theta$ -2θ scan of wurtzite MgZnO (002) plane (a); and  $\phi$ -scan of wurtzite MgZnO (101) plane (b).

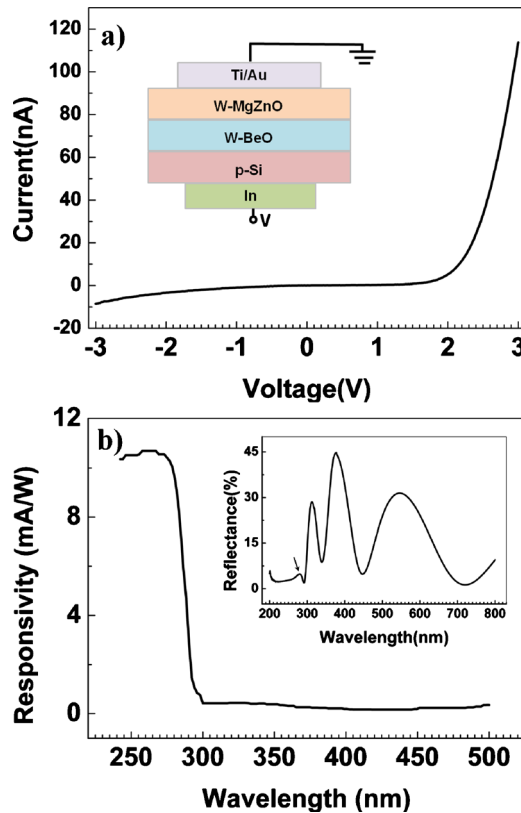


FIG. 4. (Color online) The current-voltage ( $I$ - $V$ ) characteristic of the photodetector based on n-MgZnO (0001)/p-Si (111) heterostructure. The inset provides the detailed device structure of the photodetector (a); photoreponse spectrum of the photodetector based on the n-MgZnO (0001)/p-Si (111) heterojunction at 0.5 V bias. The inset is the reflectance spectrum of the corresponding sample measured at room temperature and the black arrow indicates the band gap position (b).

MgZnO (002) planes. Importantly, the appearance of only (002) related peak combined with the RHEED findings confirms the single wurtzite phase without any sign of cubic MgZnO. In addition, Fig. 3(b) shows the  $\phi$ -scan result of MgZnO (101) plane which was carried out at around  $\chi = 60.87^\circ$  [the angle between (002) and (101) planes in a hexagonal system]. Six sharp peaks with  $60^\circ$  apart can be clearly seen, indicating a common sixfold symmetry of single wurtzite crystal structure consistent with the *in situ* RHEED observations.

Based on this p-n heterojunction, a solar-blind UV photodetector was fabricated using Ti (10 nm)/Au (50 nm) as front contact and In as back contact, respectively, as illustrated by the inset of Fig. 4(a). Semiconductor parameter analyzer (Keithley 6487) was employed for  $I$ - $V$  characterization. Figure 4(a) shows the  $I$ - $V$  curve of the p-n heterostructure, where a typical rectifying characteristic was observed with a large rectification ratio of  $\sim 300$  at  $\pm 3$  V. Moreover, the reverse dark current is lower than 2 nA at  $-3$  V. These results suggest the good interface quality and device performance of our n-MgZnO/p-Si p-n heterojunction. Photoreponse measurements were performed using the SpectraPro-500i (Acton Research Corporation) optical system with a Xe-arc lamp combined with a monochromator as the light source. The photoresponse spectrum at 0.5 V bias is demonstrated in Fig. 4(b). A sharp cutoff at wavelength of 280 nm can be recognized obviously, which corresponds to the near band absorption of the MgZnO epilayer determined from the

reflectance spectrum [as indicated by a black arrow in the inset of Fig. 4(b)]. It should be noted that no response to the visible region can be detected due to the efficient block of photogenerated holes in Si by the valence band offset, indicating a superior device performance among Si-based solar-blind UV detectors.

In summary, single-phase wurtzite MgZnO film with a solar-blind band gap was synthesized on p-Si (111) substrate by using Be and BeO layers to control the interface between Si and oxides. A photodetector was fabricated on this high-quality heterojunction with a sharp cutoff wavelength at 280 nm, demonstrating a good response to solar-blind UV radiation. An important contribution of present work is that the whole growth temperature can be lowered to 400 °C, implying a great prospect of integrating solar-blind UV optoelectronic devices with the well-developed Si microelectronic technologies. In addition, the Be (0001)/Si (111) interface was found very stable at a high temperature, and the BeO layer serves as an excellent template for the epitaxial growth of wurtzite films, opening a wide prospect to fabricate high-quality oxides on Si wafers.

This work was supported by the National Science Foundation (Grant Nos. 61076007, 50532090, 60606023, 50825206, and 10974235), the Ministry of Science and Technology (Grant Nos. 2007CB936203, 2009CB929400, 2009AA033101, and 2011CB302002) of China, the Chinese Academy of Sciences, and the Diffusion Scattering Station in Beijing Synchrotron Radiation Facility. L.G. acknowledges the financial support from the “Hundred Talents” program of the Chinese Academy of Sciences.

- <sup>1</sup>G. Parish, S. Keller, P. Kozodoy, J. P. Ibbetson, H. Marchand, P. T. Fini, S. B. Fleischer, S. P. DenBaars, U. K. Mishra, and E. J. Tarsa, *Appl. Phys. Lett.* **75**, 247 (1999).
- <sup>2</sup>M. Liao, Y. Koide, and J. Alvarez, *Appl. Phys. Lett.* **90**, 123507 (2007).
- <sup>3</sup>Y. N. Hou, Z. X. Mei, Z. L. Liu, T. C. Zhang, and X. L. Du, *Appl. Phys. Lett.* **98**, 103506 (2011).
- <sup>4</sup>X. L. Du, Z. X. Mei, Z. L. Liu, Y. Guo, T. C. Zhang, Y. N. Hou, Z. Zhang, Q. K. Xue, and A. Yu. Kuznetsov, *Adv. Mater. (Weinheim, Ger.)* **21**, 4625 (2009).
- <sup>5</sup>Y. Nishimoto, K. Nakahara, D. Takamizu, A. Sasaki, K. Tamura, S. Akasaka, H. Yuji, T. Fujii, T. Tanabe, H. Takasu, A. Tsukazaki, A. Ohtomo, T. Onuma, S. F. Chichibu, and M. Kawasaki, *Appl. Phys. Express* **1**, 091202 (2008).
- <sup>6</sup>Z. L. Liu, Z. X. Mei, T. C. Zhang, Y. P. Liu, Y. Guo, X. L. Du, A. Hallen, J. J. Zhu, and A. Yu. Kuznetsov, *J. Cryst. Growth* **311**, 4356 (2009).
- <sup>7</sup>M. Brandt, M. Lange, M. Stolzel, A. Muller, G. Benndorf, J. Zippel, J. Lenzner, M. Lorenz, and M. Grundmann, *Appl. Phys. Lett.* **97**, 052101 (2010).
- <sup>8</sup>W. Yang, S. S. Hullavarad, B. Nagaraj, I. Takeuchi, R. P. Sharma, and T. Venkatesan, *Appl. Phys. Lett.* **82**, 3424 (2003).
- <sup>9</sup>M. Fujita, M. Sasajima, Y. Deesirapipat, and Y. Horikoshi, *J. Cryst. Growth* **278**, 293 (2005).
- <sup>10</sup>C. Jin, W. Wei, H. Zhou, T.-H. Yang, and R. J. Narayan, *Appl. Phys. Lett.* **93**, 251102 (2008).
- <sup>11</sup>K. Koike, K. Hama, I. Nakashima, G.-y. Takada, K.-i. Ogata, S. Sasa, M. Inoue, and M. Yano, *J. Cryst. Growth* **278**, 288 (2005).
- <sup>12</sup>M. Razeghi and A. Rogalski, *J. Appl. Phys.* **79**, 7433 (1996).
- <sup>13</sup>C. Jin, R. Narayan, A. Tiwari, H. Zhou, A. Kvit, and J. Narayan, *Mater. Sci. Eng., B* **117**, 348 (2005).
- <sup>14</sup>N. Kawamoto, M. Fujita, T. Tatsumi, and Y. Horikoshi, *Jpn. J. Appl. Phys., Part 1* **42**, 7209 (2003).
- <sup>15</sup>X. N. Wang, Y. Wang, Z. X. Mei, J. Dong, Z. Q. Zeng, H. T. Yuan, T. C. Zhang, and X. L. Du, *Appl. Phys. Lett.* **90**, 151912 (2007).
- <sup>16</sup>M. H. Xie, S. M. Seutter, W. K. Zhu, L. X. Zheng, H. Wu, and S. Y. Tong, *Phys. Rev. Lett.* **82**, 2749 (1999).
- <sup>17</sup>Y. Sawai, K. Hazu, and S. F. Chichibu, *J. Appl. Phys.* **108**, 063541 (2010).